



# Use of [<sup>18</sup>F]FDG/PET to access the rosmarinic acid anti-inflammatory effect in a mouse sponge implant model

Schirmer, B. G. A<sup>a</sup>; Dornelas, I.C.D<sup>a</sup>; Ferreira, L. de C. A<sup>a</sup>; Marques, J. V. R<sup>a</sup>; Souza, M. D<sup>a</sup>; Miranda, M. B. de<sup>b</sup>; Castro, P. R<sup>b</sup>; Pereira, J. M<sup>b</sup>; Barcelos, L. S<sup>b</sup>; Malamut\*, C<sup>a</sup>.

<sup>a</sup> Centro de Desenvolvimento da Tecnologia Nuclear (CDTN), Unidade de Pesquisa e Produção de Radiofármacos, Av. Antônio Carlos 6.627, Campus da UFMG, Pampulha, 31270-901, Belo Horizonte, Minas Gerais, Brazil. malamut@cdtn.br.

<sup>b</sup> Department of Physiology, Biological Science Institute, Universidade Federal de Minas Gerais, Belo Horizonte, Brazil.

\*Correspondence: carlosmalamut@gmail.com

**Abstract:** Positron emission tomography (PET) is one of the most sensitive and effective imaging techniques for detecting very low concentrations of specific radiotracers. It is suitable for analyzing biochemical, metabolic, physiological and functional information at the molecular level *in vivo* and non-invasively. PET using 2-deoxy-2[<sup>18</sup>F]-fluoro-D-glucose ([<sup>18</sup>F]FDG) can be used to identify sites of inflammation and other pathologies and to monitor the efficacy of treatment. This technique can be used to study the effect of rosmarinic acid (RA) in various preclinical models. RA is a natural compound with promising antioxidant and anti-inflammatory effects. Therefore, the aim of this study is to investigate the anti-inflammatory potential of RA and the efficacy of PET/[<sup>18</sup>F]FDG in localizing inflammation and assessing response to treatment. A sponge implant model in mice was used for this purpose. All experiments were performed with male BALB/c mice aged 6 to 9 weeks and weighing 18 to 22 g, with 5 animals per group (10 animals in total throughout the study). Methods: The mice were implanted with sponge-like polyurethane discs to induce local inflammation. The animals were divided into two experimental groups: those treated with a vehicle and those treated with RA. PET scans with [<sup>18</sup>F]FDG were performed to evaluate the inflammatory process. Results: The results obtained with [<sup>18</sup>F]FDG showed a decrease in inflammatory cell infiltrates in the sponge after treatment with RA. Conclusion: The use of [<sup>18</sup>F]FDG demonstrated its efficacy in quantitatively evaluating the inflammatory process in the mouse subcutaneous sponge model as well as the anti-inflammatory effect of RA.

**Keywords:** MicroPET, [<sup>18</sup>F]FDG, anti-inflammatory agents, rosmarinic acid, sponge model.



# Uso do [ $^{18}\text{F}$ ]FDG/PET para avaliar o efeito anti-inflamatório do ácido rosmarínico em modelo murino de implante de esponja

**Resumo:** A tomografia por emissão de pósitrons (PET) é uma das técnicas de imagem mais sensíveis e eficazes para detectar concentrações muito baixas de radiotraçadores específicos. É adequado para analisar informações bioquímicas, metabólicas, fisiológicas e funcionais em nível molecular in vivo e de forma não invasiva. PET utilizando 2-desoxi-2[ $^{18}\text{F}$ ]-fluoro-D-glicose ([ $^{18}\text{F}$ ]FDG) pode identificar focos inflamatórios e outras patologias, bem como monitorar a eficácia do tratamento. Esta técnica pode ser utilizada para estudar o ácido rosmarínico (AR), um composto natural com efeitos antioxidantes e antiinflamatórios promissores. Assim, o objetivo deste estudo é investigar o potencial antiinflamatório do AR e a eficácia do PET/[ $^{18}\text{F}$ ]FDG na localização da inflamação e na avaliação da resposta ao tratamento. Para tanto, foi utilizado um modelo de implante de esponja murina. Todos os experimentos foram realizados com camundongos BALB/c machos, entre 6 e 9 semanas de idade, pesando entre 18 e 22 g, com 5 animais por grupo (totalizando 10 animais ao longo do estudo). **Metodologia:** Os ratos foram implantados com discos de poliuretano semelhantes a esponjas para induzir inflamação local. Os animais foram divididos em dois grupos experimentais: os tratados com veículo e os tratados com AR. PET scans com [ $^{18}\text{F}$ ]FDG foram realizados para avaliar o processo inflamatório. **Resultados:** Os resultados obtidos com [ $^{18}\text{F}$ ]FDG mostraram diminuição dos infiltrados de células inflamatórias na esponja após tratamento com AR. **Conclusão:** O uso de [ $^{18}\text{F}$ ]FDG demonstrou sua eficácia na avaliação quantitativa do processo inflamatório no modelo de esponja subcutânea de camundongo, bem como no efeito antiinflamatório da AR.

**Palavras-chave:** MicroPET, [ $^{18}\text{F}$ ]FDG, agentes antiinflamatórios, ácido rosmarínico, modelo de esponja.

## 1. INTRODUCTION

Positron emission tomography (PET) with [ $^{18}\text{F}$ ]FDG indicates local glucose metabolic activity and is well-known for its application in cancer diagnosis, staging, and therapy response [1]. However, [ $^{18}\text{F}$ ]FDG uptake is not entirely specific to tumor cells; various benign infectious and inflammatory processes can also result in focal radiopharmaceutical uptake [2]. The ability of Positron Emission Tomography (PET) with [ $^{18}\text{F}$ ]FDG to identify sites of inflammation is mainly related to the glycolytic activity of the cells involved in the inflammatory response [3]. Activation of immune cells is associated with increased glucose consumption to generate energy and biosynthetic precursors [4]. In this context, increased [ $^{18}\text{F}$ ]FDG uptake is a hallmark of inflammation since immune cells express high levels of glucose transporters and hexokinase activity [5]. Therefore, its preclinical application in inflammation needs to be further promoted, as well as the use of this radiopharmaceutical to evaluate the effectiveness of anti-inflammatory agents *in vivo*.

Among the promising anti-inflammatory agents, rosmarinic acid (RA) stands out. RA is a water-soluble phenolic compound originally isolated from the rosemary plant (*Rosmarinus officinalis*). *In vitro* and *in vivo* studies have shown its antioxidant, anti-inflammatory, and anti-angiogenic effects [6, 7]. For example, its anti-inflammatory effect has been observed in some animal models of neuroinflammation [8] and in a model of acute and systemic inflammation in rats [9]. Additionally, our research group demonstrated that RA at a concentration of 20 mg/kg was effective in reducing inflammation and exhibited an anti-tumor effect in the 4T1 breast tumor murine model [10]. Given its effectiveness, it is relevant to investigate the application of [ $^{18}\text{F}$ ]FDG/PET as a tool for the non-invasive study of the inflammatory process and the therapeutic response to RA treatment. This approach is justified by the lack of comprehensive preclinical studies in the

literature that evaluate the effects of RA through [ $^{18}\text{F}$ ]FDG/PET, emphasizing the need to fully understand its therapeutic potential and possible limitations.

For such investigation, the mouse sponge implant model could be useful. The mouse sponge implant model is a commonly used experimental model to study the role of new drugs in inflammation. PET imaging with this model is simple and promising for evaluating the specificity of radiopharmaceuticals because it shows all inflammatory features and components from the onset of the process to its resolution [11]. In this model, subcutaneous implantation of a sponge disc induces a chronic granulomatous response, including intense angiogenesis and an infiltrate of inflammatory cells-components present in all inflammatory processes [12]. Therefore, the sponge implant model has been used to study several drugs with angiogenic and inflammatory actions, as well as to evaluate the role of components involved in the inflammatory and vascular aspects of granuloma formation [13, 14].

Thus, this study aimed to evaluate the anti-inflammatory potential of RA and the specificity and efficiency of [ $^{18}\text{F}$ ]FDG/PET in localizing inflammation in a sponge implant model in mice.

## 2. MATERIALS AND METHODS

### 2.1. Materials

[ $^{18}\text{F}$ ]FDG was provided by the Nuclear Technology Development Center (CDTN, Belo Horizonte, Brazil) following standard procedures approved by the Brazilian National Health Surveillance Agency – ANVISA. Rosmarinic acid was purchased from Sigma-Aldrich, USA.

## 2.2. Animals

All experiments were conducted using male BALB/c mice, aged 6 to 9 weeks, and weighing 18 to 22 grams. A total of 10 mice were used in the study, divided into two groups (N=5/group). Male mice were chosen to avoid the variable of hormonal interference. The mice were obtained from the Central Animal Facility of the Federal University of Minas Gerais (CEBIO/UFMG, Belo Horizonte, Brazil). They were housed in ventilated shelves with controlled light and temperature, and had free access to food and water. Efforts were made to minimize unnecessary suffering. Animal care protocols followed the guidelines of the National Council for Control in Animal Experiments (CONCEA). This study was approved by the Nuclear Technology Development Center Animal Experimentation Committee (Protocol 002/17).

## 2.3. Preparation and implantation of sponge discs

Polyurethane sponge discs, each with a thickness of 5 mm and a diameter of 8 mm, were used as a matrix to induce local inflammation. The sponge discs were sterilized by boiling in distilled water and then soaked overnight in 70% (v/v) ethanol prior to implantation. The animals were anesthetized with a mixture of ketamine (100 mg/kg) and xylazine (10 mg/kg). The dorsal hair was shaved, and the exposed skin was wiped with 70% ethanol. The sponge discs were implanted aseptically into a subcutaneous pouch created by a 3 cm dorsal midline incision. This method minimizes the disruptive influence of the wound incision on the implant. The incisions were closed with silk-braided, non-absorbable sutures. Lidocaine was administered to the incision region through a topical ointment. Implants from ten mice were removed on day 10 after implantation to analyze inflammatory markers for acute inflammatory processes (myeloperoxidase [MPO] and N-acetyl- $\beta$ -D-glucosaminidase [NAG]), as previously described [15].

## 2.4. Rosmarinic acid treatment

The animals were randomly divided into two experimental groups: vehicle (saline-treated) and RA-treated group. RA was dissolved in saline and administered orally (20 mg/kg/day). The choice of RA dose was based on previous studies [10, 16]. Saline was administered in the vehicle-treated group. RA was administered daily from the day of implantation until the day of animal euthanasia, 10 days after sponge implantation. The animals were weighed weekly to correct for the administered doses.

## 2.5. Positron emission tomography (PET) imaging

A small animal PET system (LabPET4 Solo, GE Healthcare Technologies, Chicago, USA) with an axial length of 3.75 cm was used to acquire PET images and perform semi-quantitative analysis (Standard Uptake Values, SUV). The acquisition of [<sup>18</sup>F]FDG images was performed 7 days after sponge implantation, based on a previous study [17]. The animals were fasted for at least 4 hours, anesthetized with 2% isoflurane in 100% oxygen, administered 10–14 MBq [<sup>18</sup>F]FDG, and scanned 60 minutes after intravenous injection. The animals were scanned sequentially, with an acquisition time of 15 minutes each. They were kept warm and anesthetized in the prone position during acquisition. Image reconstruction was performed using the maximum likelihood expectation maximization (MLEM) method in 3D with 40 iterations. A normalization file was used for the reconstruction. A phantom image was acquired to determine the calibration factor for the device. Volume-of-interest (VOI) analysis of the reconstructed images was performed using PMOD® software (Version 3.3). A standard VOI was created and applied to all images. The VOI was placed around the sponge implant and the limb muscles, which were adopted as normal tissue with baseline uptake. Sponge-to-muscle SUV ratios (Averaged SUV, sponge/SUV muscle) were calculated. N-Acetyl-β-D-glucosaminidase and myeloperoxidase activity measurement

The animals were euthanized by cervical dislocation after peritoneal anesthesia with a mixture of ketamine (100 mg/kg) and xylazine (10 mg/kg) on day 10 post-implantation for inflammatory cell analysis on the sponge samples. The effects of RA treatment on macrophage and neutrophil accumulation in the sponge were estimated by measuring myeloperoxidase (MPO) and N-Acetyl- $\beta$ -D-glucosaminidase (NAG) enzyme activities, as previously described [10].

## 2.6. Hemoglobin dosage

The measurement of intra-implant hemoglobin content indirectly quantifies the neovascularization present in the tissue and has been used as an index of vascularization in angiogenesis models. The sponge discs were carefully removed from the animals, weighed, and homogenized in 2.0 ml of a Drabkin reagent (Labtest, São Paulo, Brazil) using a tissue homogenizer (Tekmar TR-10, Ohio, USA) and centrifuged at 10,000 rpm for 40 minutes at 4° C. The supernatants were then filtered through 0.22 $\mu$ m membranes (Millipore) and placed in 96-well plates. Readings were taken spectrophotometrically at 540 nm and the hemoglobin concentration was determined by comparison with a standard hemoglobin curve. The results obtained were expressed as hemoglobin concentration (microgram) per milligram of wet weight of the implant.

## 2.7. Sponge image analysis

Images of the sponge (10 days after implantation) were analyzed using the software ImageJ and the Color Histogram plug-in, downloaded from the NIH website (<http://rsb.info.nih.gov/ij>). The initial color analysis to detect the red color range was designed as a positive to evaluate the relative intensity of the color of the sponges. The calculations were based on the absolute intensity values of the sponge collected after the experiment and the absolute intensity value of the standard sponge (before implantation) that followed the calculations.  $\text{Relative Intensity} = \text{Absolute Intensity (collected sponge)} \div \text{Absolute Intensity (standard sponge)}$ .

## 2.8. Statistical analysis

Statistical analysis was performed using GraphPad Prism 6.0 (Graphpad Software Inc., USA). Results are expressed as means  $\pm$  standard deviation. Student's t-tests were used to compare the two groups. Statistical significance was set at  $P < 0.05$ .

## 3. RESULTS AND DISCUSSIONS

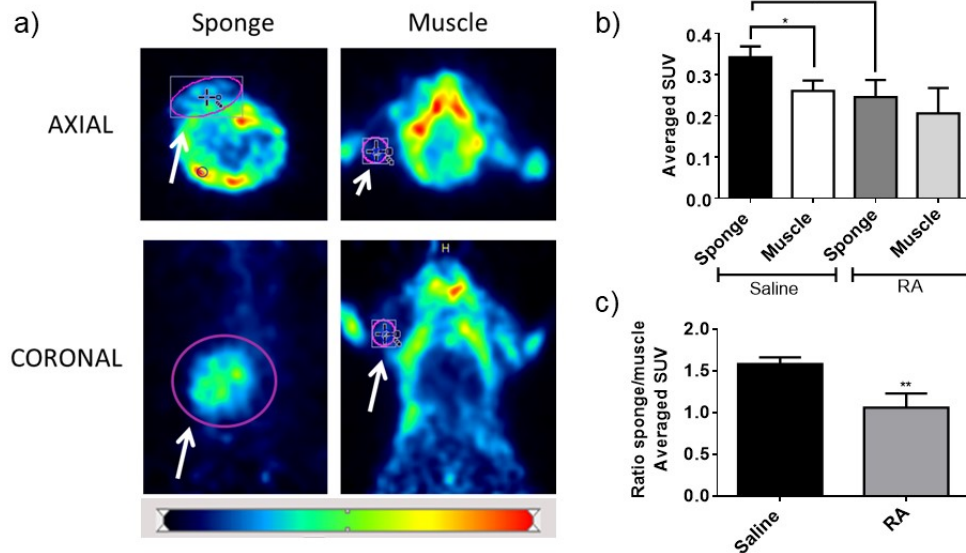
### 3.1. [<sup>18</sup>F]FDG/PET imaging of sponge implant model

Polyurethane sponge discs were used as a matrix to induce local inflammation. After implantation of the sponge, treatment with RA was given and [<sup>18</sup>F]FDG/PET imaging was performed on day 7. Standard VOIs were placed in these regions to compare the [<sup>18</sup>F]FDG image in the sponge and in the muscle, a non-inflamed tissue (Fig. 1A). An increase in [<sup>18</sup>F]FDG uptake was observed in the sponge region of the control group compared to the muscle (Fig. 1B). On the other hand, [<sup>18</sup>F]FDG uptake after RA treatment was similar to that in muscle (Fig. 1B). The sponge/muscle ratio shows that the uptake in the sponge after RA treatment was significantly lower than in the muscle (Fig. 1C).

The effects of RA are reported in previous studies mainly due to its interference in the cellular and molecular pathways of the anti-inflammatory response. According to Cao and colleagues [18], treatment with RA promotes antiadipogenic and anti-inflammatory activity. RA attenuates inflammatory responses in lipopolysaccharide-induced mastitis in mice by inhibiting pathways like NF- $\kappa$ B and MAPKs. It also shows protective effects in acute liver injury and atopic dermatitis models, further demonstrating its broad anti-inflammatory potential [19].



**Figure 1:** [ $^{18}\text{F}$ ]FDG image of sponge-implanted animals (a) Representative images indicating the positioning of VOIs in the sponge and muscle 7 days after sponge implantation in Balb/c male mice. (b) Quantification of [ $^{18}\text{F}$ ]FDG uptake in sponge and muscle region (SUV). (c) Quantification of the sponge/muscle ratio. Results were expressed as Mean  $\pm$  SD of 5 animals in each group. \* $p < 0.05$ , \*\* $p < 0.01$  compared with muscle uptake of [ $^{18}\text{F}$ ]FDG or saline group using Student's t-test.



Therefore, it is possible to observe in Figure 1A that after 7 days of sponge implantation, there was a reduction in the uptake of [ $^{18}\text{F}$ ]FDG in the RA-treated group. The parameters analyzed in graphs 1B and 1C suggest that RA treatment reduced [ $^{18}\text{F}$ ]FDG uptake in the sponge, showing a similarity between [ $^{18}\text{F}$ ]FDG uptake in the sponge to the muscle. Suggesting the anti-inflammatory effect of RA treatment. A previous study carried out by our research group also suggests the anti-inflammatory and neuroprotective effects of RA in a murine model of cerebral ischemia and reperfusion [16].

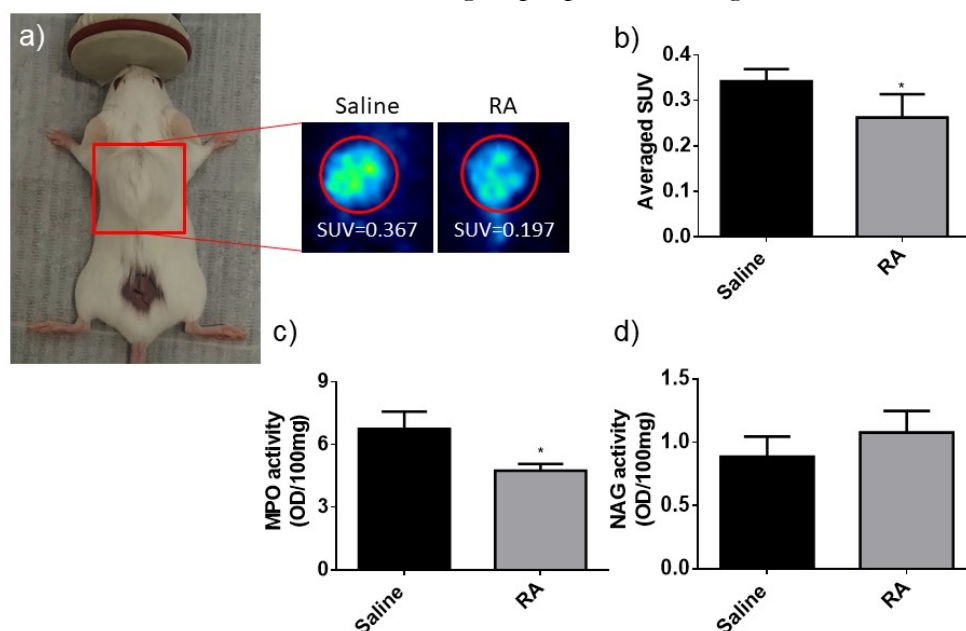
### 3.2. Effect of RA on inflammatory cell infiltrate in the sponge

The sponge discs were implanted into a subcutaneous pouch in the dorsal region of the animals (Fig. 2a). It was observed that the [ $^{18}\text{F}$ ]FDG uptake was significantly lower in the RA-treated group than in the saline-treated group (Fig. 2b). The sponge implant is a stimulus that triggers the cascade of inflammatory events that can increase glucose consumption of [ $^{18}\text{F}$ ]FDG through inflammation and cell proliferation. RA-treated mice had reduced MPO

levels, indicating a lower presence of neutrophils in the sponge (Fig. 2c), and there was no statistical difference in NAG levels compared to the saline group (Fig. 2d).

Previous studies have demonstrated the effects of RA and its anti-inflammatory properties in mouse models. As described by [18], RA has effects not only on reducing the overproduction of IL-1 $\beta$ , IL-6, and TNF- $\alpha$  but also on suppressing the expressions of p65 and p-p65 compared to a model of mice carrying H22, in the tumor microenvironment. Furthermore, studies by [20] also demonstrate through *in vivo* and *in vitro* experiments that RA has an inhibitory effect on the proliferation and adhesion of endothelial cells and the development of tumor angiogenesis. These results strongly suggest an important role for the anti-inflammatory effect of RA in inhibiting the proliferation and migration of 4T1 tumor cells. Interestingly, Pereira *et al.*, (2023), also encouraged that daily treatment with RA at a dose of 20 mg/kg reduces the neutrophil infiltrate and does not alter the presence of macrophages in the primary tumor [10].

**Figure 2 :** [ $^{18}\text{F}$ ]FDG uptake and inflammatory cells in the sponge (a) Representative images of [ $^{18}\text{F}$ ]FDG, 7 days after sponge implantation in Balb/c male mice. The area highlighted in red indicates the implanted region of the sponge. (b) Quantification of [ $^{18}\text{F}$ ]FDG uptake in the sponge of RA and saline-treated group (SUV). (c) MPO and (d) NAG levels in the sponge of control (saline) and RA-treated groups, 10 days after sponge implantation, expressed as optical density (OD) per 100 mg of tissue. Results were expressed as Mean  $\pm$  SD of 5 animals in each group. \* $p < 0.05$  using Student's t-test.

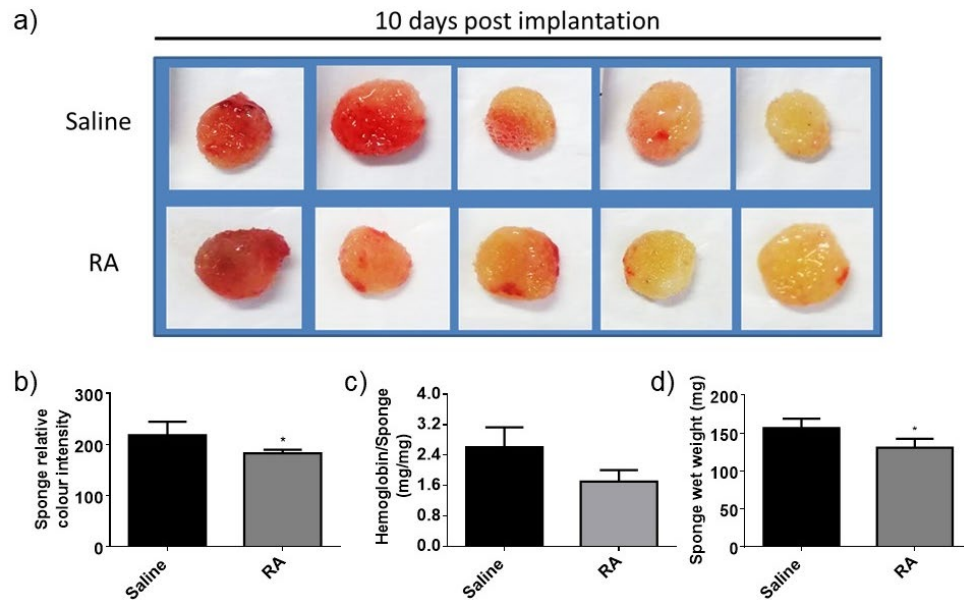


Therefore, the inflammatory process caused by the sponge can be seen in Fig. 2a. It is possible to observe that RA treatment performed every day reduced the uptake of [ $^{18}\text{F}$ ]FDG compared to the saline group. The parameters analyzed in the graphs of Fig. 2b, 2c and 2d indicate that RA-treated mice had lower SUV, MPO and NAG levels. These results confirm the anti-inflammatory effect of RA. Interestingly, in a previous study, we demonstrated that FDG uptake in 4T1 breast tumors was reduced in the RA-treated group, which significantly affected the inflammatory response. This study showed a reduction in mast cells and neutrophils (by NAG) in the primary tumor and macrophages (by MPO) in the lungs, along with reduced tumor angiogenesis [10].

### 3.3. Effect of RA on angiogenesis

The results obtained with [ $^{18}\text{F}$ ]FDG/PET indicated a reduction in inflammatory cell infiltrates in the sponge after treatment with RA, which could be due to reduced angiogenesis. Angiogenesis, the process of formation of new blood vessels, can be observed in the sponge in the second week after implantation (Fig. 3a). The intensity of color (Fig. 3b), hemoglobin content (Fig. 3c) and weight of the sponges (Fig. 3d) were lower in the group of RA-treated animals, suggesting vascularization.

**Figure 3:** RA effect on angiogenesis (a) Representative images of sponge 10 days after sponge implantation. (b) Quantification of red color intensity in the sponge of RA and saline-treated group. (c) Hemoglobin quantification in the sponge (d) Wet weight in the sponge of control (saline) and RA-treated groups. Results were expressed as Mean  $\pm$  SD of 5 animals in each group. \* $p < 0.05$  using Student's t-test.



The anti-inflammatory effects of rosmarinic acid, both locally and systemically, are well-documented in mouse models, as described in the study by Rocha *et al.*, (2015). In the sponge implantation model in mice, angiogenic and inflammatory responses can be quantified *in vivo*, with new blood vessel formation triggered by the inflammatory processes generated by the implant [9, 12, 21]. This model serves as a basis for evaluating the efficacy of new therapies, such as rosmarinic acid, in the present study.

Therefore, similar morphological changes in the sponges can be seen in Figure 3a with a reduction in infiltrates after 10 days of implantation in the control group and the RA group. The parameters analyzed in graphs 3b, 3c, and 3d suggest a reduction in vascularization in the group of animals treated with RA. These results support the ability of RA to modulate angiogenesis, which is consistent with the intrinsic relationship between neovascularization and inflammatory processes. These results thus confirm the anti-inflammatory effect of the phenolic compound and are consistent with the reduced formation of blood vessels in these implants. In another experimental model, our group

has shown *in vivo* and *in vitro* experiments that RA inhibits the development of tumor angiogenesis [10].

## 4. CONCLUSIONS

The present study demonstrated that treatment with RA acts to reduce MPO levels, and also showed a reduction in the uptake of [<sup>18</sup>F]FDG/PET. In conclusion, the use of [<sup>18</sup>F]FDG demonstrated, on the one hand, its potential to quantitatively evaluate the inflammatory process generated in the subcutaneous murine sponge model and, on the other, the anti-inflammatory action of rosmarinic acid in the sponge model. Therefore, the use of [<sup>18</sup>F]FDG/PET associated with the sponge model is a non-invasive strategy for the study of new anti-inflammatory agents. Additionally, for greater experimental control and obtaining better results, it is recommended that glucose be measured before and after the image.

## ACKNOWLEDGMENT

We thank the staff and all collaborators of the Production and Radiopharmaceutical Research Unit and the group of the Molecular Imaging Laboratory and Bioassay Laboratory of CDTN/CNEN.

## FUNDING

This research was supported by the Nuclear Technology Development Center (CNEN).

## CONFLICT OF INTEREST

All authors declare that they have no conflicts of interest.

## REFERENCES

- [1] Li, Y., Wang, Q., Wang, X., Li, X., Wu, H., Wang, Q., & Li, X. F. (2020). Expert Consensus on clinical application of FDG PET/CT in infection and inflammation. *Annals of Nuclear Medicine*, 34, 369-376.
- [2] RAHMAN, W. T. et al. The impact of infection and inflammation in oncologic 18F-FDG PET/CT imaging. **Biomedecine & pharmacotherapie [Biomedicine & pharmacotherapy]**, v. 117, n. 109168, p. 109168, 2019.
- [3] JAMAR, F. et al. EANM/SNMMI guideline for<sup>18</sup>F-FDG use in inflammation and infection. **Journal of Nuclear Medicine**, v. 54, n. 4, p. 647–658, 2013.
- [4] CALDER, P. C.; DIMITRIADIS, G.; NEWSHOLME, P. Glucose metabolism in lymphoid and inflammatory cells and tissues. **Current opinion in clinical nutrition and metabolic care**, v. 10, n. 4, p. 531–540, 2007.
- [5] MARTINEAU, P. et al. Assessing cardiovascular infection and inflammation with FDG-PET. **American Journal of Nuclear Medicine and Molecular Imaging**, v. 11, n. 1, p. 46, 2021.
- [6] QIAO, S. et al. Rosmarinic acid inhibits the formation of reactive oxygen and nitrogen species in RAW264.7 macrophages. **Free radical research**, v. 39, n. 9, p. 995–1003, 2009.
- [7] YOUN, J. et al. Beneficial effects of rosmarinic acid on suppression of collagen induced arthritis. **The journal of rheumatology**, v. 30, n. 6, 2003.
- [8] LUAN, H. et al. Rosmarinic acid protects against experimental diabetes with cerebral ischemia: relation to inflammation response. **Journal of neuroinflammation**, v. 10, n. 1, 2013.
- [9] ROCHA, J. et al. Anti-inflammatory effect of rosmarinic acid and an extract of *Rosmarinus officinalis* in rat models of local and systemic inflammation. **Basic & clinical pharmacology & toxicology**, v. 116, n. 5, p. 398–413, 2015.

- [10] PEREIRA, J. M. et al. Use of [18F]FLT/PET for assessing the tumor evolution and monitoring the antitumor activity of rosmarinic acid in a mouse 4T1 breast tumor model. **Brazilian Journal of Radiation Sciences**, v. 11, n. 3, p. 01–23, 2023.
- [11] FARIA ALMEIDA, F. A. DE et al. KETO[18F]FDG -VAP-P1: In vivo studies of a potential PET radiotracer for diagnosis of inflammation. **Applied radiation and isotopes: including data, instrumentation and methods for use in agriculture, industry and medicine**, v. 192, n. 110547, p. 110547, 2023.
- [12] CASTRO, P. R. et al. Kinetics of implant-induced inflammatory angiogenesis in abdominal muscle wall in mice. **Microvascular research**, v. 84, n. 1, p. 9–15, 2012.
- [13] FERREIRA, M. A. N. D. et al. Sponge-induced angiogenesis and inflammation in PAF receptor-deficient mice (PAFR-KO). **British journal of pharmacology**, v. 141, n. 7, p. 1185–1192, 2004.
- [14] GUABIRABA, R. et al. Blockade of cannabinoid receptors reduces inflammation, leukocyte accumulation and neovascularization in a model of sponge-induced inflammatory angiogenesis. **et al [Inflammation research]**, v. 62, n. 8, p. 811–821, 2013.
- [15] CASSINI-VIEIRA, P. et al. Estimation of wound tissue neutrophil and macrophage accumulation by measuring myeloperoxidase (MPO) and N-acetyl- $\beta$ -D-glucosaminidase (NAG) activities. **Bio-protocol**, v. 5, n. 22, 2015.
- [16] SANTOS, E. V. DOS et al. Applicability of [18F]FDG/PET for investigating rosmarinic acid preconditioning efficacy in a global stroke model in mice. **Brazilian Journal of Pharmaceutical Sciences**, v. 59, p. e21555, 2023.
- [17] LANNA, M. F. et al. Kinetics of phenotypic and functional changes in mouse models of sponge implants: Rational selection to optimize protocols for specific biomolecules screening purposes. **Frontiers in bioengineering and biotechnology**, v. 8, 2020.
- [18] CAO, W. et al. Rosmarinic acid inhibits inflammation and angiogenesis of hepatocellular carcinoma by suppression of NF- $\kappa$ B signaling in H22 tumor-bearing mice. **Journal of pharmacological sciences**, v. 132, n. 2, p. 131–137, 2016.
- [19] JIANG, K. et al. Anti-inflammatory effects of rosmarinic acid in lipopolysaccharide-induced mastitis in mice. **Inflammation**, v. 41, n. 2, p. 437–448, 2018
- [20] HUANG, S.-S.; ZHENG, R.-L. Rosmarinic acid inhibits angiogenesis and its mechanism of action in vitro. **Cancer letters**, v. 239, n. 2, p. 271–280, 2006.

- [21] ANDRADE, S. P.; FERREIRA, M. A. N. D. The sponge implant model of angiogenesis. Em: **Methods in Molecular Biology**. New York, NY: Springer New York, 2016. v. 1430p. 333–343.

---

## LICENSE

This article is licensed under a Creative Commons Attribution 4.0 International License, which permits use, sharing, adaptation, distribution and reproduction in any medium or format, as long as you give appropriate credit to the original author(s) and the source, provide a link to the Creative Commons license, and indicate if changes were made. The images or other third-party material in this article are included in the article's Creative Commons license, unless indicated otherwise in a credit line to the material.

To view a copy of this license, visit <http://creativecommons.org/licenses/by/4.0/>.